Coherent Electronic Wave Packet Motion in C_{60} Controlled by the Waveform and Polarization of Few-Cycle Laser Fields

H. Li,[1,2,3] B. Mignolet,[4] G. Wachter,[5] S. Skruszewicz,[6] S. Zherebtsov,[1,2] F. Süßmann,[1,2] A. Kessel,[1] S. A. Trushin,[1] Nora G. Kling,[2,3] M. Kübel,[1,2] B. Ahn,[1,7,8] D. Kim,[7,8] I. Ben-Itzhak,[3] C. L. Cocke,[3] T. Fennel,[6] J. Tiggesbäumker,[6] K.-H. Meiwes-Broer,[6] C. Lemell,[5] J. Burgdörfer,[5,9] R. D. Levine,[10,11] F. Remacle,[4] and M. F. Kling[1,2,3]

[1]*Max Planck Institute of Quantum Optics, Garching D-85748, Germany*
[2]*Department of Physics, Ludwig-Maximilians-Universität München, Garching D-85748, Germany*
[3]*J.R. MacDonald Laboratory, Physics Department, Kansas State University, Manhattan, Kansas 66506, USA*
[4]*Department of Chemistry, University of Liège, Liège B-4000, Belgium*
[5]*Institute for Theoretical Physics, Vienna University of Technology, Vienna A-1040, Austria*
[6]*Institute of Physics, Universität Rostock, Rostock D-18051, Germany*
[7]*Physics Department, CASTECH, POSTECH, Pohang, Kyungbuk 790-784, Republic of Korea*
[8]*Max Planck Center for Attosecond Science, Max Planck POSTECH/KOREA Research Initiative, Pohang 790-784, Republic of Korea*
[9]*Institute of Nuclear Research of the Hungarian Academy of Sciences (ATOMKI), Debrecen H-4001, Hungary*
[10]*Fritz Haber Center for Molecular Dynamics, Hebrew University of Jerusalem, Jerusalem 91904, Israel*
[11]*Department of Chemistry and Biochemistry, University of California Los Angeles, Los Angeles, California 90095, USA*

(Received 12 September 2014; published 27 March 2015)

Strong laser fields can be used to trigger an ultrafast molecular response that involves electronic excitation and ionization dynamics. Here, we report on the experimental control of the spatial localization of the electronic excitation in the C_{60} fullerene exerted by an intense few-cycle (4 fs) pulse at 720 nm. The control is achieved by tailoring the carrier-envelope phase and the polarization of the laser pulse. We find that the maxima and minima of the photoemission-asymmetry parameter along the laser-polarization axis are synchronized with the localization of the coherent electronic wave packet at around the time of ionization.

DOI: 10.1103/PhysRevLett.114.123004 PACS numbers: 33.80.Eh, 31.15.xv, 42.50.Hz, 71.20.Tx

Electrons determine the forces on the nuclei in molecules. Tuning the nonequilibrium electronic dynamics before the onset of significant nuclear motion opens new routes for tailoring chemical reactivity. For few-cycle optical pulses, varying the phase between the envelope and the field amplitude [carrier-envelope phase (CEP)] can be used to control electronic dynamics induced in molecules during the interaction with the pulse [1–3]. Electronic dynamics are typically probed indirectly by recording molecular fragmentation patterns of dissociative (ionization) channels exploiting the coupling between the electronic and nuclear degrees of freedom [4–26]. The analysis of the fragmentation patterns is usually complex—even for simple diatomic molecules—and quickly becomes prohibitively complicated for large polyatomic molecules because of the large number of fragmentation channels [3]. Angularly resolved photoionization by ultrashort laser pulses has been advocated for probing the electronic dynamics before the onset of significant nuclear motion (see, e.g., [27–31]).

Fullerenes are nanometer-size systems with interesting physical properties, including high polarizability [32], superatomic molecular orbitals [33,34] with macroatom behavior [35], large photoionization cross sections [36,37], and efficient high-harmonic generation [38–40]. The ionization and fragmentation of C_{60} have been investigated extensively in the past (see, e.g., [35,41–47]). C_{60} is very stable and is one of the few molecular systems for which the ionization energy is smaller than the lowest fragmentation threshold. Therefore it is an ideal system for probing electronic dynamics, and, when suitably excited, the electronic density oscillates on a nanometer scale. Moreover, in the experiments reported here, the pulse duration is short enough to avoid significant thermionic emission that occurs for longer pulse durations of hundreds of femtoseconds to nanoseconds [48,49]. In this Letter, we demonstrate the control over transient electronic dynamics in a large polyatomic system, the C_{60} fullerene, and we find that the angular distribution of direct photoelectrons reflects the spatial localization of the electronic wave packet at about the time of ionization.

The electron emission from C_{60} as a function of the CEP is recorded with phase-tagged velocity-map imaging (VMI) [50]. Details of the experimental setup are contained in the Supplemental Material [51]. The few-cycle laser pulses are focused into the VMI chamber where they intersect a molecular beam of C_{60}, generated by heating high-purity C_{60} powder in a home-built oven. Measured 2D-momentum images correspond to projections along the spectrometer axis (p_z). Linear polarized (LP) pulses are polarized along the y axis and circular polarized (CP) pulses in the yz plane. The CEP is measured by a single-shot phase meter [65,66] and the absolute CEP was determined from Xe reference scans.

Quantum dynamical (QD) and classical Monte Carlo (MC) trajectory simulations were used to theoretically investigate the CEP-dependent electron emission from C_{60}. Both calculation methods are described in the Supplemental Material [51] and briefly in the following. In our QD simulations, the photoionization and photoexcitation electronic dynamics induced by a short laser pulse are computed by numerically solving the time-dependent Schrödinger equation using a coupled equation scheme including bound and ionized states. The bound states are described in a basis of 407 electronic states of C_{60} (i.e., all states below the ionization threshold). The acceleration and deceleration of the continuum electron by the electric field, and thus the scattering dynamics, are accounted for. The angular distribution of a continuum electron with a given momentum depends on the coherently excited bound states at the instant of ionization and their coupling to the continuum. Thus, by varying the polarization and the CEP of the pulse, the time-dependent wave packet evolves differently, which is reflected in the angular distribution of the photoelectrons [30,31,67–69]. The electron spectra are computed by integrating the population of the ionized states at the end of the pulse. The calculations have been focal-volume averaged (in the two dimensions perpendicular to the laser propagation) for comparison to the experimental data.

We complement our QD calculations with MC simulations of electron emission and rescattering in analogy to the simple man's model [70]. Such simulations have been successfully used for the description of electron emission and rescattering for atoms for both LP [71,72] and CP [73,74] and have been generalized to electron emission from nanoparticles [75] and from metal nanostructures [76,77].

Experimentally obtained CEP-integrated electron momentum images for LP and CP at the same laser field amplitude of 22.1 GV m^{-1} corresponding to a cycle-averaged peak intensity of 6.5×10^{13} W cm^{-2} and 1.3×10^{14} W cm^{-2}, respectively, are shown in Figs. 1(a)–1(c). Figures 1(d) and 1(e) show the computed and experimental ionization yield as a function of the radial momentum p_r, defined as $p_r = \sqrt{p_x^2 + p_y^2}$. Contributions from both direct and rescattered electrons can be distinguished by the MC simulations. For LP, rescattered electrons dominate the signal above $p_r = 0.6$ a.u. For CP, the rescattered electrons only start to dominate the total signal around 1.3 a.u. The high-momentum cutoff, corresponding to an energy of about $10U_p$, where U_p is the ponderomotive potential, is in both cases around 1.5 a.u. The QD-simulated photoelectron spectra diverge from the measured data in the low-momentum region. This is due to the fact that the Coulomb interaction between the ionized electron and the cationic core is not well represented due to our use of a plane wave basis to describe the continuum electron, which leads to a lower photoelectron yield at low momenta. At very low kinetic energies the QD simulations underestimate the contribution of ionization from deeply bound states, which are, however, quickly depopulated within the pulse.

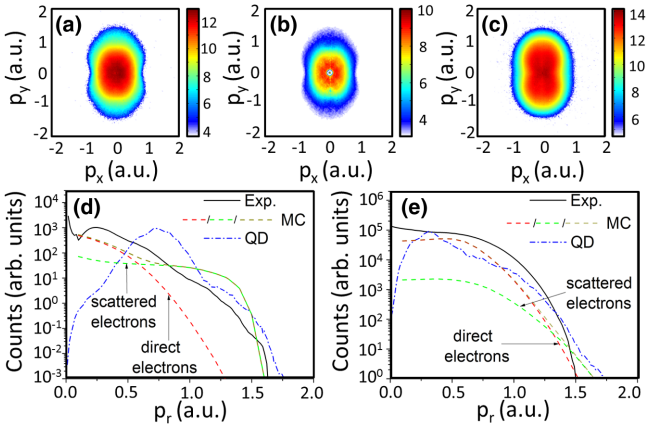

FIG. 1 (color online). Recorded CEP-averaged electron momentum image (projected along p_z) from C_{60} with (a) LP at $(6.5 \pm 0.5) \times 10^{13}$ W cm^{-2} and (c) CP at $(1.3 \pm 0.1) \times 10^{14}$ W cm^{-2}. For LP, a cut at $p_z = 0$ through the 3D-momentum distribution, obtained after inversion [78], is shown in (b). Experimental and theoretical photoelectron spectra (PES) of C_{60} with (d) LP and (e) CP obtained from angular integration of (b) and (c), respectively (the scales of the vertical axes are logarithmic). Contributions from direct and rescattered electrons were obtained from the MC simulations (dashed red and green lines). The full PES from MC and QD simulations are shown as dashed brown and dash-dotted blue lines, respectively. All simulation data were obtained for the experimental field strengths taking volume averaging into account.

In Figs. 2(a) and 2(b) we show the amplitude and phase of the CEP-dependent electron yield for LP and CP. In order to obtain the graphs, we integrated the CEP-dependent yields over p_x, p_y using 0.02 a.u. × 0.02 a.u. bins. The integrated yields are parameterized as a sinusoidal $N(\varphi) = N_0 \sin(\varphi + \varphi_0)$, where N_0 is the amplitude and φ_0 denotes a phase offset. The parameters N_0 and φ_0 are shown as a function of p_x and p_y in Figs. 2(a) and 2(b). A CEP-dependent yield with a nearly constant amplitude and phase for the highest discernible direct electrons is found within the range of momenta marked by a solid red line. This range is contained within an angle of about ±15° along the polarization axis. For the same angular range, the region of the rescattering electrons close to the cutoff is marked by a solid black line.

The CEP and momentum dependence of the directional electron emission from C_{60} for both LP and CP are analyzed via the asymmetry parameter, defined as

$$A(\mathbf{p}, \varphi) = \frac{N_{+y}(\mathbf{p}, \varphi) - N_{-y}(\mathbf{p}, \varphi)}{N_{+y}(\mathbf{p}, \varphi) + N_{-y}(\mathbf{p}, \varphi)}, \quad (1)$$

where $\mathbf{p}$ is the momentum vector of the continuum electron, $N_{+y}(\mathbf{p}, \varphi)$ and $N_{-y}(\mathbf{p}, \varphi)$ represent the yield of

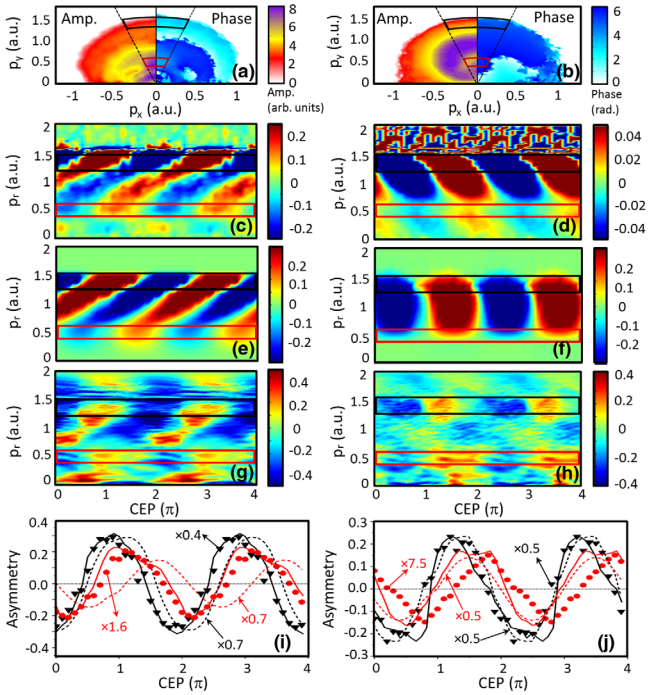

FIG. 2 (color online). Momentum-dependent amplitude (left half) and phase (right half) of the CEP-dependent oscillation in the photoelectron yield for (a) LP and (b) CP. Because of $-p_x$, p_x symmetry, only one quarter is shown. Angular-integrated asymmetry maps obtained from the (c),(d) experimental, (e),(f) MC, and (g),(h) QD simulation results for LP and CP, respectively. (i),(j) Comparison between angle- and momentum-integrated asymmetries from experiment for high-momentum electrons (band with $1.3 \leq p_r \leq 1.5$, black triangles) and low-momentum electrons ($0.4 \leq p_r \leq 0.6$, red circles), QD computations (solid black and red curves), and MC simulations (dotted black and red curves) obtained from panels (c)–(h) above. For better comparison of phase shifts in the oscillatory behavior, the experimental and MC curves were multiplied by the indicated factors.

the continuum electrons in the $+y$ and $-y$ direction, respectively, and φ is the CEP. The asymmetry typically shows an oscillatory behavior with CEP [79]. A strong variation of the asymmetry parameter indicates a large degree of control, which results from the short, near-single cycle pulses. Integration of the momentum images over the angular ranges indicated in Figs. 2(a) and 2(b) yields the experimental asymmetry maps as a function of radial momentum and φ in Figs. 2(c) and 2(d), which we compare to the theoretical data in Figs. 2(e)–2(h).

For LP and CP [Figs. 2(c)–2(h)] characteristic differences can be discerned between low-momentum electrons ($p_r \leq 0.6$ a.u.) corresponding to direct ionization and high-momentum electrons ($p_r \geq 0.6$ a.u.) corresponding to rescattered electrons for LP. In the high-momentum region the predictions by both classical and quantum dynamical simulations agree well with the experimental data in periodicity and phase shifts with p_r. This is further supported by the comparison of the asymmetries integrated over a selected range of high momenta ($1.3 \leq p_r \leq 1.5$ a.u.), see Figs. 2(i) and 2(j). The amplitudes differ here by only about a factor of 2 between the results.

In contrast to the generally good agreement between experiment and theory at high momenta, for a band in the low-momentum region ($0.4 \leq p_r \leq 0.6$ a.u.), chosen to be at the highest discernible momenta for direct electrons in LP, the classical simulations exhibit a strong phase shift with respect to the experimental data for LP. This indicates that the direct electron emission is not accurately described within the MC simulations. In contrast, the QD simulations reproduce accurately the phase of the asymmetry and its magnitude semiquantitatively. Moreover, these simulations provide insights on the relation between the anisotropy and the bound-states dynamics. Our interpretation is as follows: The angular distribution of the photoelectrons and, therefore, the asymmetry parameter depends on the shape and localization of the transiently formed bound-state wave packet as well as its coupling to the continuum. While the photoionization coupling elements vary with the electron momentum (magnitude and direction) but are independent of the electric field strength, the bound-state wave packet dynamics strongly depend on the pulse characteristics such as the CEP, the strength of the electric field, and the polarization. The variation of the asymmetry parameter as a function of CEP for the direct ionization is thus controlled by the motion of the wave packet modulated by the momentum-dependent coupling elements.

The time-dependent electron densities for LP and CP obtained from the QD simulations are depicted in Fig. 3. The pulse induces complex transient dynamics resulting in collective electron motion. At the beginning of the pulse, the ground state is efficiently excited by multiphoton transitions to the higher states. When the electric field reaches its maximum, close to $t = 3.5$ fs, the ionization rate steeply increases [see Figs. 3(a) and 3(b)]. At each time, and depending on the value of the CEP, ionization from a different superposition of the ground state and transient excited states occurs, leading to a different angular distribution of the continuum electron.

The evolutions of the bound electron dynamics are reflected by the dipole moments, shown in Figs. 3(c) and 3(d) for LP and CP, respectively. They follow the electric field almost adiabatically at the beginning of the pulse, until ionization occurs. The excited states are accessed by multiphoton transitions. At the field maximum, the electronic states ionize and subsequently the dipole moment collapses. For $\varphi = 0$, the electron density is mainly localized on the bottom of the molecule (in the $-y$ direction) at $t = 3.5$ fs [Fig. 3(e)], when the photoionization probability is maximum since direct ionization is more probable where the electron density is the largest. For this CEP, the asymmetry parameter is negative for low (< 0.6 a.u.) momentum [see Fig. 2(i)], which corresponds to a preferential ionization of the electrons in the $-y$

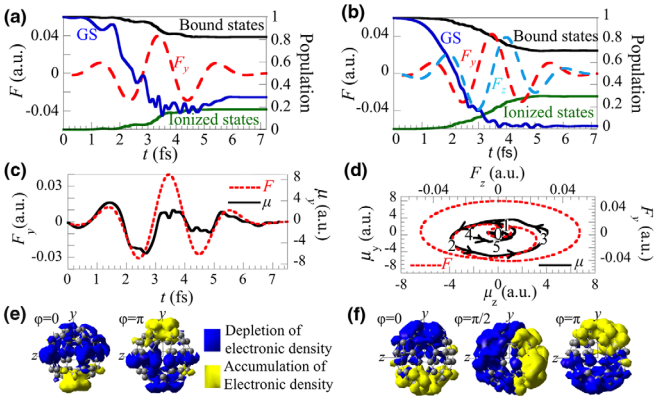

FIG. 3 (color online). (a),(b) Time-dependent population of the ground state (GS), bound, and ionized states for LP (a) and CP (b) ($\varphi = 0$). For LP, the dipole oscillates along the direction of the electric field (c) while for CP (d), the dipole undergoes a spiraling motion as a function of time (shown on the dipole curve). At the maximum of the pulse ($t = 3.5$ fs), when the ionization reaches a maximum, the electronic density is localized in a different part of the molecule depending on the CEP. The isocontour difference ($0.0003|e|/\text{Å}^3$) between the density at the time $t = 3.5$ fs and $t = 0$ fs are shown for several CEP for LP (e) and CP (f). The full time dependence of the density difference is provided in the Supplemental Material [51] as a movie.

direction. For pulses with $\varphi = \pi$, the direction is reversed. We find that about 0.3 of the one-electron density is transferred from the top of the molecule to the bottom. Therefore, we infer that by tailoring the CEP, it is possible to control the spatial localization of the electron density at a given time during the pulse.

For CP the dipole undergoes a spiraling motion as a function of time and only goes back to zero at the end of the pulse, as shown in Fig. 3(d) for $\varphi = 0$. The electron density differences between $t = 3.5$ fs and $t = 0$ fs for CP with $\varphi = 0$, $\pi/2$, and π are depicted in Fig. 3(f). They demonstrate the directional control of the bound electronic density with the CEP.

The observed asymmetries in the rescattering region above 0.6 a.u. show a rightward tilt with increasing momentum for LP and a leftward tilt for CP (see Fig. 2). The rightward tilt for LP has been previously observed for other atomic and molecular targets and can be assigned to the correlation between recollision energy and recollision time [80–82].

In the experiments with CP we observe a pronounced leftward tilt of the asymmetry, indicating that electrons with high momenta are advanced with respect to the field rotation direction compared to electrons with lower momenta. The leftward tilt of the asymmetry is reproduced by both QD and MC simulations. Analysis of trajectories from our MC simulations reveals that the advancement of high-momentum electrons is linked to a rescattering process involving a sequence of small-angle collisions specific to more complex systems such as C_{60}.

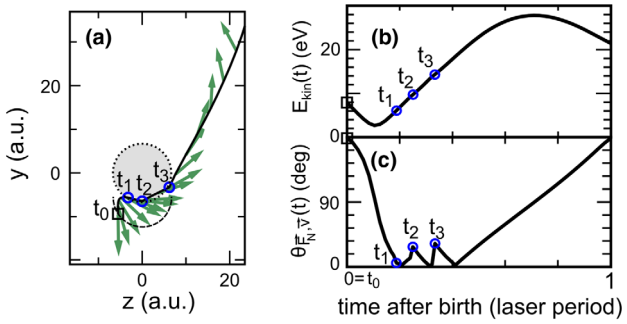

FIG. 4 (color online). (a) Typical rescattering trajectory (black solid line) for circular polarization [time-dependent laser-induced force $\mathbf{F}_N(t) = -\mathbf{F}(t)$, green vectors, scaled] starting from the classical tunnel exit (dashed line) at t_0 (square). Scattering events (blue circles, times t_1 to t_3) occur at the C_{60} shell (dotted circle). (b) Kinetic energy $E_{\text{kin}}(t) = |\mathbf{v}(t)|^2/2$. (c) Angle $\theta_{\mathbf{F}_N,\mathbf{v}}(t)$ between velocity $\mathbf{v}(t)$ and laser force.

The leftward tilt is observed for electrons gaining high momenta ($p \gtrsim 1$ a.u.) in the CP laser field. For the latter to occur, the instantaneous momentum vector should stay aligned with the laser induced force $\mathbf{F}_N(t) = -\mathbf{F}(t)$ during the rescattering process (Fig. 4). This subset of trajectories involves electrons taking off from the tunneling exit towards the target and undergoing typically two to three small-angle collisions at atoms of the C_{60} shell, thereby rotating the velocity vector in tune with the rotation of the CP laser field. The electrons eventually emerge with momentum vector p_{final} pointing in the direction opposite to that of their initial position vector and that of the electric force vector $\mathbf{F}_N(t_{\text{tunnel}})$ at the tunnel exit. This 180° rotation differs from the 90° rotation between $\mathbf{F}_N(t_{\text{tunnel}})$ and $\mathbf{p}_{\text{final}} = \int_{t_{\text{tunnel}}}^{\infty} \mathbf{F}_N(t)dt$ for circularly polarized light in the absence of rescattering. It is this advancement that leaves its mark as the leftward tilt in the asymmetry spectrum. The MC simulations indicate that about 1% of the trajectories lead to scattering and most of the electrons that reach high momenta undergo a sequence of small-angle rescatterings.

This particular recollision mechanism differs from the conventional laser-induced rescattering for atomic or diatomic molecules, where circular polarization strongly quenches electron (back)scattering. Backscattering with high energy gain via multiple small-angle collisions in elliptical or circular polarization will likely also play a role in other extended targets such as large molecules, clusters, nanoparticles, and droplets.

In conclusion, the polarization and the CEP of intense few-cycle laser pulses were used to demonstrate the spatiotemporal control of electronic wave packet motion in C_{60}. The CEP-dependent asymmetry of the electron emission at high momenta can be understood from simple classical arguments, where the influence of the vector potential on the trajectory of the continuum electron needs to be taken into account. Furthermore, the classical simulations indicate that the leftward tilt of the asymmetry of

the rescattered electrons for CP is caused by a series of small-angle collisions with the C_{60} shell. At low momenta, direct ionization dominates, and from our QD simulations we infer that the asymmetry parameter reflects the localization of the coherently excited electron density at about the time of ionization. Similar trends are expected to be observed in other fullerenes under comparable laser conditions. Furthermore, the spatiotemporal control demonstrated here can be extended to other systems, such as clusters or nanoparticles, that undergo collective electron dynamics when exposed to a strong field.

We acknowledge S. Karsch and F. Krausz for their support of the PFS/AS-5 infrastructure and S. Nagele for fruitful discussions. We are grateful for support by the Max Planck Society and the DFG via SFB652/3 and the Cluster of Excellence: Munich Centre for Advanced Photonics (MAP). H. L. and M. F. K. acknowledge support in the early stages of this project by the Chemical Sciences, Geosciences, and Biosciences Division, Office of Basic Energy Sciences, Office of Science, U.S. Department of Energy (Grant No. DE-SC0008146). JRML personnel were supported by the same funding agency (Grant No. DE-FG02-86ER13491). B. A. and D. K. acknowledge support from National Research Foundation of Korea (NRF) funded by Ministry of Science, ICT and Future Planning via Global Research Laboratory Program (Grant No. 2009-00439), and Max Planck POSTECH/KOREA Research Initiative Program (Grant No. 2011-0031558). This work was supported by the FWF (Austria), SFB-041 ViCoM, SFB-049 Next Lite, and P21141-N16. H. L. and G. W. thank the International Max Planck Research School of Advanced Photon Science for financial support. Calculations were performed using the Vienna Scientific Cluster (VSC). B. M. and F. R. gratefully acknowledge support from Fonds National de la Recherche and from Fonds National de la Recherche Collective of Belgium (Grant No. 2.4545). F. R. and R. D. L. gratefully acknowledge support from the Einstein Foundation (Berlin).

[1] F. Lépine, G. Sansone, and M. J. J. Vrakking, Chem. Phys. Lett. **578**, 1 (2013).
[2] M. F. Kling, P. von den Hoff, I. Znakovskaya, and R. de Vivie-Riedle, Phys. Chem. Chem. Phys. **15**, 9448 (2013).
[3] F. Lépine, M. Y. Ivanov, and M. J. J. Vrakking, Nat. Photonics **8**, 195 (2014).
[4] V. Roudnev, B. D. Esry, and I. Ben-Itzhak, Phys. Rev. Lett. **93**, 163601 (2004).
[5] M. F. Kling, Science **312**, 246 (2006).
[6] I. Barth, J. Manz, Y. Shigeta, and K. Yagi, J. Am. Chem. Soc. **128**, 7043 (2006).
[7] X. M. Tong and C. D. Lin, Phys. Rev. Lett. **98**, 123002 (2007).
[8] F. He, C. Ruiz, and A. Becker, Phys. Rev. Lett. **99**, 083002 (2007).
[9] D. Geppert, P. von den Hoff, and R. de Vivie-Riedle, J. Phys. B **41**, 074006 (2008).
[10] M. Kremer, B. Fischer, B. Feuerstein, V. L. B. de Jesus, V. Sharma, C. Hofrichter, A. Rudenko, U. Thumm, C. D. Schröter, R. Moshammer *et al.*, Phys. Rev. Lett. **103**, 213003 (2009).
[11] I. Znakovskaya, P. von den Hoff, S. Zherebtsov, A. Wirth, O. Herrwerth, M. J. J. Vrakking, R. de Vivie-Riedle, and M. F. Kling, Phys. Rev. Lett. **103**, 103002 (2009).
[12] B. Fischer, M. Kremer, T. Pfeifer, B. Feuerstein, V. Sharma, U. Thumm, C. D. Schröter, R. Moshammer, and J. Ullrich, Phys. Rev. Lett. **105**, 223001 (2010).
[13] K. P. Singh, F. He, P. Ranitovic, W. Cao, S. De, D. Ray, S. Chen, U. Thumm, A. Becker, M. M. Murnane *et al.*, Phys. Rev. Lett. **104**, 023001 (2010).
[14] G. Sansone, F. Kelkensberg, J. F. Perez-Torres, F. Morales, M. F. Kling, W. Siu, O. Ghafur, P. Johnsson, M. Swoboda, E. Benedetti *et al.*, Nature (London) **465**, 763 (2010).
[15] F. Kelkensberg, G. Sansone, M. Y. Ivanov, and M. Vrakking, Phys. Chem. Chem. Phys. **13**, 8647 (2011).
[16] P. von den Hoff, R. Siemering, M. Kowalewski, and R. de Vivie-Riedle, IEEE J. Sel. Top. Quantum Electron. **18**, 119 (2012).
[17] X. Zhou, P. Ranitovic, C. W. Hogle, J. H. D. Eland, H. C. Kapteyn, and M. M. Murnane, Nat. Phys. **8**, 232 (2012).
[18] W. Siu, F. Kelkensberg, G. Gademann, A. Rouzée, P. Johnsson, D. Dowek, M. Lucchini, F. Calegari, U. De Giovannini, A. Rubio *et al.*, Phys. Rev. A **84**, 063412 (2011).
[19] I. Znakovskaya, P. von den Hoff, G. Marcus, S. Zherebtsov, B. Bergues, X. Gu, Y. Deng, M. J. J. Vrakking, R. Kienberger, F. Krausz *et al.*, Phys. Rev. Lett. **108**, 063002 (2012).
[20] F. Anis and B. D. Esry, Phys. Rev. Lett. **109**, 133001 (2012).
[21] H. Xu, J.-P. Maclean, D. E. Laban, W. C. Wallace, D. Kielpinski, R. T. Sang, and I. V. Litvinyuk, New J. Phys. **15**, 023034 (2013).
[22] N. G. Kling, K. J. Betsch, M. Zohrabi, S. Zeng, F. Anis, U. Ablikim, B. Jochim, Z. Wang, M. Kübel, M. F. Kling *et al.*, Phys. Rev. Lett. **111**, 163004 (2013).
[23] T. Rathje, A. M. Sayler, S. Zeng, P. Wustelt, H. Figger, B. D. Esry, and G. G. Paulus, Phys. Rev. Lett. **111**, 093002 (2013).
[24] E. Lötstedt and K. Midorikawa, Phys. Rev. A **88**, 041402 (2013).
[25] P. Ranitovic, C. W. Hogle, P. Rivière, A. Palacios, X.-M. Tong, N. Toshima, A. González-Castrillo, L. Martin, F. Martín, M. M. Murnane *et al.*, Proc. Natl. Acad. Sci. U.S.A. **111**, 912 (2014).
[26] H. Li, A. S. Alnaser, X. M. Tong, K. J. Betsch, M. Kübel, T. Pischke, B. Förg, J. Schötz, F. Süßmann, S. Zherebtsov *et al.*, J. Phys. B **47**, 124020 (2014).
[27] F. Remacle and R. D. Levine, Proc. Natl. Acad. Sci. U.S.A. **103**, 6793 (2006).
[28] B. Mignolet, R. D. Levine, and F. Remacle, Phys. Rev. A **86**, 053429 (2012).
[29] B. Mignolet, R. D. Levine, and F. Remacle, Phys. Rev. A **89**, 021403 (2014).
[30] K.-J. Yuan, S. Chelkowski, and A. D. Bandrauk, Chem. Phys. Lett. **592**, 334 (2014).
[31] B. Mignolet, R. D. Levine, and F. Remacle, J. Phys. B **47**, 124011 (2014).

[32] A. Ballard, K. Bonin, and J. Louderback, J. Chem. Phys. **113**, 5732 (2000).
[33] M. Feng, J. Zhao, and H. Petek, Science **320**, 359 (2008).
[34] J. O. Johansson, G. G. Henderson, F. Remacle, and E. E. B. Campbell, Phys. Rev. Lett. **108**, 173401 (2012).
[35] Y. Huismans, E. Cormier, C. Cauchy, P. A. Hervieux, G. Gademann, A. Gijsbertsen, O. Ghafur, P. Johnsson, P. Logman, T. Barillot *et al.*, Phys. Rev. A **88**, 013201 (2013).
[36] B. Mignolet, J. O. Johansson, E. E. B. Campbell, and F. Remacle, ChemPhysChem **14**, 3332 (2013).
[37] R. Völpel, G. Hofmann, M. Steidl, M. Stenke, M. Schlapp, R. Trassl, and E. Salzborn, Phys. Rev. Lett. **71**, 3439 (1993).
[38] V. R. Bhardwaj, P. B. Corkum, and D. M. Rayner, Phys. Rev. Lett. **93**, 043001 (2004).
[39] R. A. Ganeev, L. B. Elouga Bom, J. Abdul-Hadi, M. C. H. Wong, J. P. Brichta, V. R. Bhardwaj, and T. Ozaki, Phys. Rev. Lett. **102**, 013903 (2009).
[40] R. A. Ganeev, C. Hutchison, T. Witting, F. Frank, S. Weber, W. A. Okell, E. Fiordilino, D. Cricchio, F. Persico, A. Zaïr *et al.*, J. Opt. Soc. Am. B **30**, 7 (2013).
[41] M. Tchaplyguine, K. Hoffmann, O. Dühr, H. Hohmann, G. Korn, H. Rottke, M. Wittmann, I. V. Hertel, and E. E. B. Campbell, J. Chem. Phys. **112**, 2781 (2000).
[42] E. E. B. Campbell, K. Hoffmann, H. Rottke, and I. V. Hertel, J. Chem. Phys. **114**, 1716 (2001).
[43] M. Boyle, K. Hoffmann, C. P. Schulz, I. V. Hertel, R. D. Levine, and E. E. B. Campbell, Phys. Rev. Lett. **87**, 273401 (2001).
[44] M. Boyle, M. Hedén, C. P. Schulz, E. E. B. Campbell, and I. V. Hertel, Phys. Rev. A **70**, 051201 (2004).
[45] C. Bordas, B. Baguenard, B. Climen, M. A. Lebeault, F. Lépine, and F. Pagliarulo, Eur. Phys. J. D **34**, 151 (2005).
[46] I. Shchatsinin, T. Laarmann, N. Zhavoronkov, C. P. Schulz, and I. V. Hertel, J. Chem. Phys. **129**, 204308 (2008).
[47] I. V. Hertel, I. Shchatsinin, T. Laarmann, N. Zhavoronkov, H. H. Ritze, and C. P. Schulz, Phys. Rev. Lett. **102**, 023003 (2009).
[48] J. O. Johansson and E. E. B. Campbell, Chem. Soc. Rev. **42**, 5661 (2013).
[49] E. E. B. Campbell and R. D. Levine, Annu. Rev. Phys. Chem. **51**, 65 (2000).
[50] F. Süßmann, S. Zherebtsov, J. Plenge, N. G. Johnson, M. Kübel, A. M. Sayler, V. Mondes, C. Graf, E. Rühl, G. G. Paulus *et al.*, Rev. Sci. Instrum. **82**, 093109 (2011).
[51] See Supplemental Material at http://link.aps.org/supplemental/10.1103/PhysRevLett.114.123004, which includes Refs. [52–64].
[52] I. Ahmad *et al.*, Appl. Phys. B **97**, 529 (2009).
[53] J. Abrefah, D. R. Olander, M. Balooch, and W. J. Siekhaus, Appl. Phys. Lett. **60**, 1313 (1992).
[54] H. Feshbach, Ann. Phys. (N.Y.) **19**, 287 (1962).
[55] R. D. Levine, *Quantum Mechanics of Molecular Rate Processes* (Clarendon Press, Oxford, 1969).
[56] T. Yanai, D. P. Tew, and N. C. Handy, Chem. Phys. Lett. **393**, 51 (2004).
[57] J. O. Johansson, E. Bohl, G. G. Henderson, B. Mignolet, T. J. S. Dennis, F. Remacle, and E. E. B. Campbell, J. Chem. Phys. **139**, 084309 (2013).
[58] G. M. Seabra, I. G. Kaplan, V. G. Zakrzewski, and J. V. Ortiz, J. Chem. Phys. **121**, 4143 (2004).
[59] C. M. Oana and A. I. Krylov, J. Chem. Phys. **131**, 124114 (2009).
[60] E. W. Schlag and H. J. Neusser, Acc. Chem. Res. **16**, 355 (1983).
[61] R. B. Bernstein, J. Phys. Chem. **86**, 1178 (1982).
[62] D. A. Gobeli, J. J. Yang, and M. A. El-Sayed, Chem. Rev. **85**, 529 (1985).
[63] N. B. Delone and V. P. Krainov, *Multiphoton Processes in Atoms* (Springer, Berlin, 1994).
[64] F. Salvat, A. Jablonski, and C. J. Powell, Comput. Phys. Commun. **165**, 157 (2005).
[65] T. Wittmann, B. Horvath, W. Helml, M. Schätzel, X. Gu, A. L. Cavalieri, G. G. Paulus, and R. Kienberger, Nat. Phys. **5**, 357 (2009).
[66] T. Rathje, N. G. Johnson, M. Möller, F. Süßmann, D. Adolph, M. Kübel, R. Kienberger, M. F. Kling, G. G. Paulus, and A. M. Sayler, J. Phys. B **45**, 074003 (2012).
[67] C. Neidel, J. Klei, C. H. Yang, A. Rouzée, M. J. J. Vrakking, K. Klünder, M. Miranda, C. L. Arnold, T. Fordell, A. L'Huillier *et al.*, Phys. Rev. Lett. **111**, 033001 (2013).
[68] F. Remacle, M. Nest, and R. D. Levine, Phys. Rev. Lett. **99**, 183902 (2007).
[69] B. Mignolet, R. D. Levine, and F. Remacle, J. Phys. Chem. A **118**, 6721 (2014).
[70] P. B. Corkum, Phys. Rev. Lett. **71**, 1994 (1993).
[71] G. G. Paulus, W. Becker, W. Nicklich, and H. Walther, J. Phys. B **27**, L703 (1994).
[72] G. G. Paulus, W. Becker, and H. Walther, Phys. Rev. A **52**, 4043 (1995).
[73] P. Eckle, A. N. Pfeiffer, C. Cirelli, A. Staudte, R. Dörner, H. G. Muller, M. Büttiker, and U. Keller, Science **322**, 1525 (2008).
[74] A. N. Pfeiffer, C. Cirelli, M. Smolarski, R. Dörner, and U. Keller, Nat. Phys. **7**, 428 (2011).
[75] S. Zherebtsov, T. Fennel, J. Plenge, E. Antonsson, I. Znakovskaya, I. Ahmad, A. Wirth, O. Herrwerth, S. Trushin, V. Pervak *et al.*, Nat. Phys. **7**, 656 (2011).
[76] M. Krüger, M. Schenk, P. Hommelhoff, G. Wachter, C. Lemell, and J. Burgdörfer, New J. Phys. **14**, 085019 (2012).
[77] G. Wachter, C. Lemell, J. Burgdörfer, M. Schenk, M. Krüger, and P. Hommelhoff, Phys. Rev. B **86**, 035402 (2012).
[78] M. J. J. Vrakking, Rev. Sci. Instrum. **72**, 4084 (2001).
[79] V. Roudnev and B. D. Esry, Phys. Rev. Lett. **99**, 220406 (2007).
[80] G. G. Paulus, F. Lindner, H. Walther, A. Baltuška, E. Goulielmakis, M. Lezius, and F. Krausz, Phys. Rev. Lett. **91**, 253004 (2003).
[81] M. F. Kling, J. Rauschenberger, A. J. Verhoef, E. Hasović, T. Uphues, D. B. Milošević, H. G. Muller, and M. J. J. Vrakking, New J. Phys. **10**, 025024 (2008).
[82] A. Gazibegović-Busuladžić, E. Hasović, M. Busuladžić, D. B. Milošević, F. Kelkensberg, W. K. Siu, M. J. J. Vrakking, F. Lépine, G. Sansone, M. Nisoli *et al.*, Phys. Rev. A **84**, 043426 (2011).